ARTICLES

Journal of Semiconductors
(2019) 40, 122803
doi: 10.1088/1674-4926/40/12/122803

Study of the morphology evolution of AlN grown on nano-patterned sapphire substrate

Zhuohui Wu[1, 2, 3, 4], Jianchang Yan[1, 2, 3, 4, †], Yanan Guo[1, 2, 3, 4], Liang Zhang[1, 2, 3, 4], Yi Lu[1, 2, 3, 4], Xuecheng Wei[1, 2, 3, 4], Junxi Wang[1, 2, 3, 4, †], and Jinmin Li[1, 2, 3, 4]

[1]Research and Development Center for Solid State Lighting, Institute of Semiconductors, Chinese Academy of Sciences, Beijing 100083, China
[2]Center of Materials Science and Optoelectronics Engineering, University of Chinese Academy of Sciences, Beijing 100049, China
[3]Beijing Engineering Research Center for the 3rd Generation Semiconductor Materials and Application, Beijing 100083, China
[4]State Key Laboratory of Solid-State Lighting, Beijing 100083, China

Abstract: This study focused on the evolution of growth front about AlN growth on nano-patterned sapphire substrate by metal-organic chemical vapor deposition. The substrate with concave cones was fabricated by nano-imprint lithography and wet etching. Two samples with different epitaxy procedures were fabricated, manifesting as two-dimensional growth mode and three-dimensional growth mode, respectively. The results showed that growth temperature deeply influenced the growth modes and thus played a critical role in the coalescence of AlN. At a relatively high temperature, the AlN epilayer was progressively coalescence and the growth mode was two-dimensional. In this case, we found that the inclined semi-polar facets arising in the process of coalescence were $\{11\bar{2}1\}$ type. But when decreasing the temperature, the $\{11\bar{2}2\}$ semi-polar facets arose, leading to inverse pyramid morphology and obtaining the three-dimensional growth mode. The 3D inverse pyramid AlN structure could be used for realizing 3D semi-polar UV-LED or facet-controlled epitaxial lateral overgrowth of AlN.

Key words: AlN; epitaxial lateral overgrowth; growth front evolution; 2D and 3D growth modes; MOCVD

Citation: Z H Wu, J C Yan, Y N Guo, L Zhang, Y Lu, X C Wei, J X Wang, and J M Li, Study of the morphology evolution of AlN grown on nano-patterned sapphire substrate[J]. *J. Semicond.*, 2019, 40(12), 122803. http://doi.org/10.1088/1674-4926/40/12/122803

1. Introduction

High-quality AlN template is essential to fabricate high-efficiency deep-ultraviolet light-emitting diodes (LEDs) and laser diodes (LDs), which can be widely used in sterilization, water purification, medicine, and biochemistry. Sapphire is one of the most suitable substrates for high-quality AlN template, thanks to its mature processing technique and high transparency in UV-light range[1]. However, the heteroepitaxy of AlN template in sapphire substrate leads to high threading dislocation density (TDD), typically in the order of 10^9–10^{10} cm^{-2}, and deteriorates internal quantum efficiency (IQE) of the devices. Epitaxial lateral overgrowth (ELOG) on patterned sapphire substrate (PSS) or AlN/sapphire template has been proven to be an effective technique to obtain low TDD and crack-free AlN template since part of the threading dislocations would bend and get annihilated[2, 3]. Many groups used those techniques to obtain high-performance device which was benefited from high internal quantum efficiency due to the improvement of crystal quality[4–6].

Various patterns are selected to serve for the ELOG, such as stripe[3, 4, 7–17], concave cone[5, 18–20] or convex cone[21]. As for the stripe pattern, realizing coalescence of AlN has been a crucial issue. Many groups discussed the influence of stripe direction[3, 8, 9, 13], and found that if the stripe is along $\langle 11\bar{2}0\rangle_{AlN}$, the coalescence is very difficult. The other growth conditions, such as growth temperature[3, 8, 9, 12], V/III ratio[12, 16] were also optimized to obtain flat AlN. Some groups combined the ELOG with migration enhanced technique[7, 11], which is useful to accelerate the coalescence. For the convex cone pattern, which is widely used for commercial blue LED, none report has been heard that AlN can coalesce like GaN by MOCVD. However, Hagedorn *et al.*[21] realized coalescence of AlN grown on the top of the truncated cone, which is more like the coalescence of AlN rods[6, 22].

ELOG on concave patterned sapphire substrate can bring significant improvements for the crystal quality and device performance, which has reported by Dong *et al.*[5, 18]. Wang *et al.*[20] and Zhang *et al.*[19] further explored the V/III radio and pattern's size to reduce the TDD. However, the morphology evolution and coalescence mechanism of AlN grown on the concave patterned sapphire substrate has been rarely reported. In fact, coalescence mechanism of the AlN differs greatly from the GaN. The $\{11\bar{2}2\}$ facet which typically exists in the process of ELOG of GaN is almost invisible in the ELOG of AlN, unless modulating the growth temperature, which would be shown later. And purely modulating the V/III ratio could not obtain the stabilized growth of $\{11\bar{2}2\}$ facet.

It should be noted that evolution of the facets might affect the evolution of the dislocation. For instance, with reference to the ELOG of GaN, the inclined facets arising in the process of coalescence play an important role in reducing the dislocation, as the threading dislocations which terminate at the inclined facets will bend in the basal plane during the lateral growth. Consequently, two steps ELOG of GaN including

Correspondence to: J C Yan, yanjc@semi.ac.cn; J X Wang, jxwang@semi.ac.cn
Received 19 FEBRUARY 2019; Revised 24 APRIL 2019.

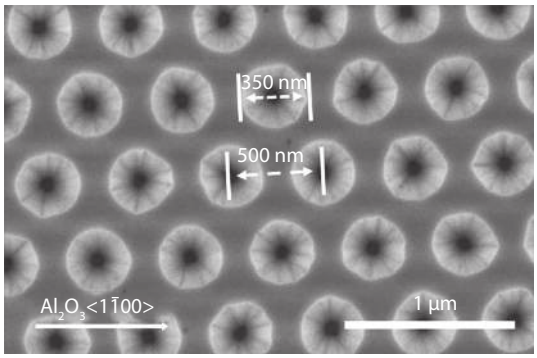

Fig. 1. Plan-view SEM image of the NPSS.

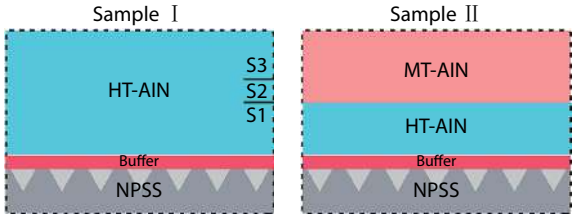

Fig. 2. (Color online) Schematic diagrams of two samples with different structures.

both 3D process which makes the surface contain as large inclined facets as possible and 2D recovery process was mentioned to improve crystal quality, which is called facet-controlled epitaxial lateral overgrowth (FACELO)[23–26]. To our knowledge, such concept has been rarely studied in the ELOG of AlN. However, as for ELOG of AlN, high-density threading dislocations might still exist above the mesa region[9, 10].

In this paper, morphology evolution of AlN growth on NPSS under different growth conditions was detailly discussed and the growth habit of the {11$\bar{2}$2} facet of AlN was reported. For the common growth conditions (high temperature and appropriate V/III ratio), the AlN has 2D growth mode. The {11$\bar{2}$1} facets arise and then vanish in the process, thus leading to coalescence. And when decreasing the temperature, the {11$\bar{2}$2} facets arise, leading to 3D growth mode. Keeping growth at the lower temperature, the (0001) *c*-plane facet vanishes and growth front entirely consists of {11$\bar{2}$2} facets, appearing to inverse pyramid AlN structure.

2. Experiment

In this research, the NPSS was fabricated by nano-imprint lithography. As shown in Fig. 1, the opening diameter of circular hole is about 350 nm, and the period of the pattern is about 500 nm. A home-made low-pressure metal–organic chemical vapor deposition (LP–MOCVD) system with a vertical shower-head reactor was used to process epitaxial growth. Trimethylaluminum (TMAl) and ammonia (NH_3) were used as precursors for Al and N, respectively. High-purity hydrogen (H_2) was used as the carrier gas. The reaction pressure was set as 50 Torr. Two samples with different structures were fabricated, as shown in Fig. 2, which manifested as different growth modes. The sample I contained the HT-AlN layers purely, which were grown at 1200 °C as normal growth temperature. The growth time for the HT-AlN in sample I was two hours, leading to near coalescence of the AlN epilayer. And the growth process of sample I was divided into three stages, which were labeled as S1 (0~40 min), S2 (40–60 min) and S3 (60–120 min), to investigate the evolution of the surface morphology. For sample II, an MT-AlN layer was grown based on the HT-AlN layer at 1130 °C. The growth time for the both HT-AlN layer and MT-AlN layer in sample II was 40 min. In addition, the V/III ratios of the HT-AlN and MT-AlN were 578 and 1156, respectively. Both samples were grown based on low-temperature buffer layer at 790 °C. The growth rate of HT-AlN and MT-AlN under the abovementioned growth condition was about 1.2 μm/h. After growth, scanning electron microscopy (SEM) and atomic force microscope (AFM) were used to study the surface morphology of the AlN.

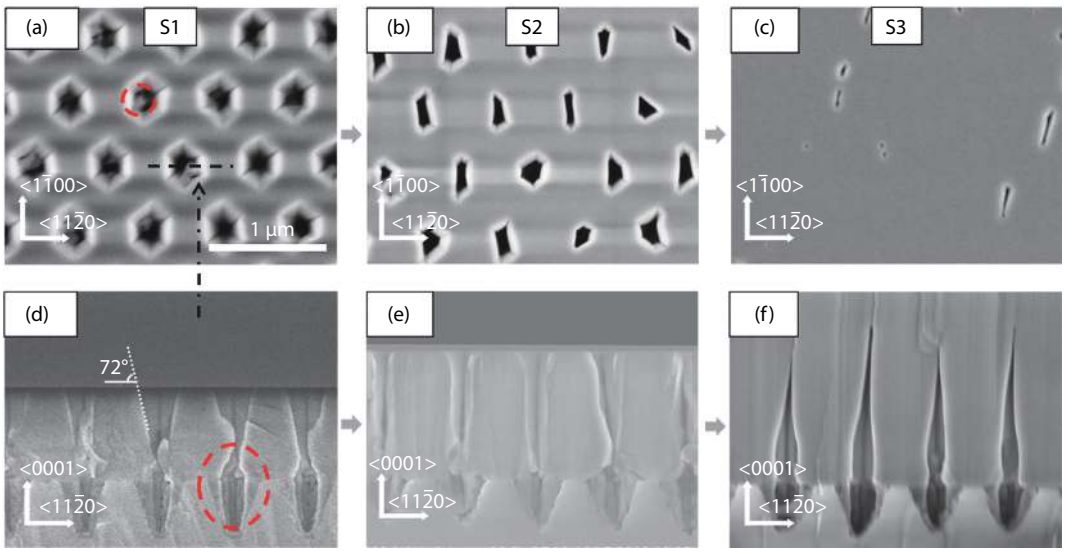

Fig. 3. (a–c) Plan-view SEM images of surface morphology of sample I at end of the three growth stages. (d–f) The corresponding cross-sectional SEM images for (a), (b) and (c). The black dashed line in (a) indicates direction of the cross-sectional view as (d), (e) and (f). All images use the same scale bar as (a).

3. Results and discussion

Fig. 3 presents the morphology of three distinguishing stages of Sample I. The corresponding growth time was 40, 60, and 120 min, respectively. At the initial stage, locally con-

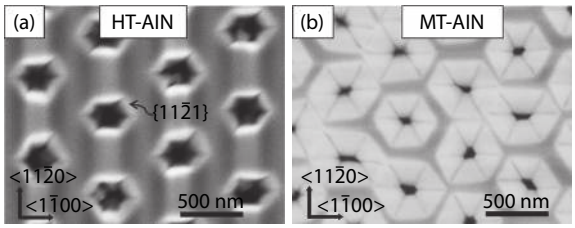

Fig. 4. Plan-view SEM images of surface morphology of Sample II.

tinuous AlN film with circular holes was gradually formed above un-etched mesa zones of the substrate after hundreds-nanometer growth. Then the outer contour of the holes turned into a hexagon shape when thickness of the AlN is around 800 nm, as shown in Fig. 3(a). Six inclined {11$\bar{2}x$} facets were exposed, due to the lateral growth of the AlN. The angle θ between the {11$\bar{2}x$} facets and the (0001) facet (*c*-plane) is determined by following equation

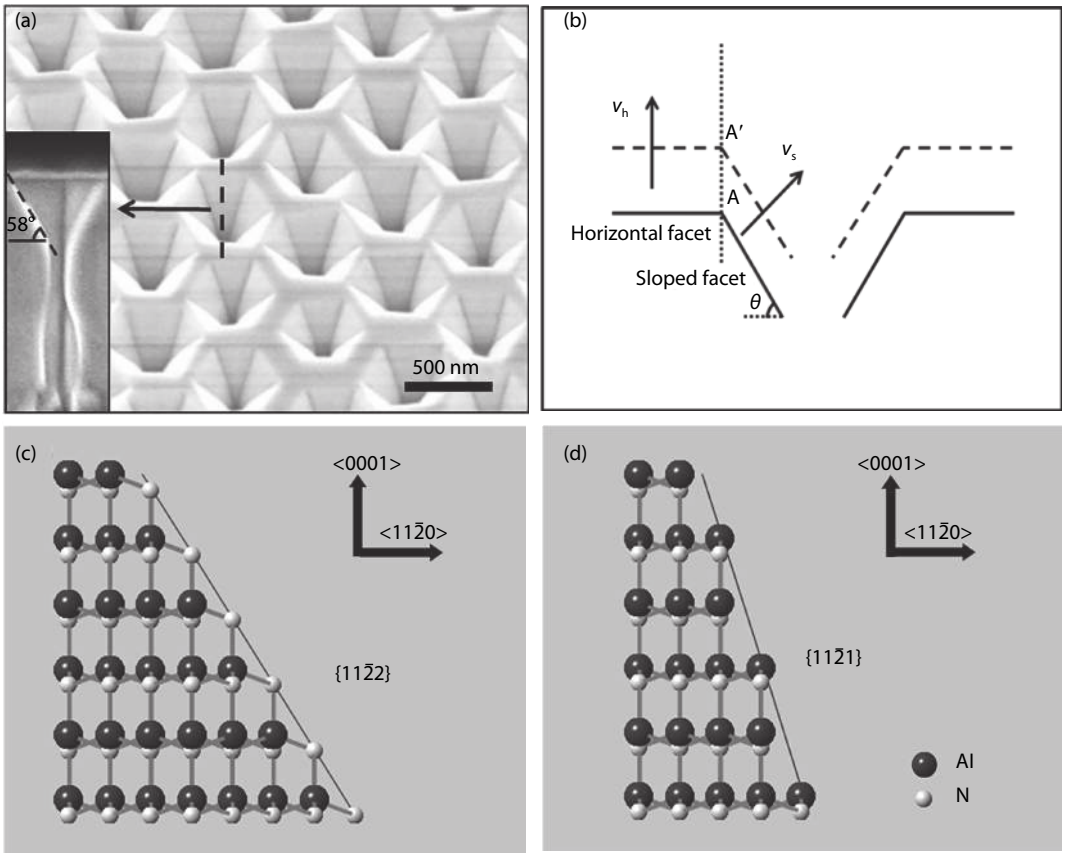

Fig. 5. (a) 25° tilted-view SEM image of surface morphology of for as-grown MT-AlN. The inset shows cross-sectional view with the direction indicated by the black dashed line. (b) Schematic diagram of AlN growth keeping the 3D morphology. (c) and (d) Schematic of the AlN atomic structure.

$$\theta = \tan^{-1}\left(\frac{2c}{xa}\right).$$

As shown in Fig. 3(d), the value of θ is around 72°, thus the value of x is deduced to be ~1. According to the Wulff growth theory[27], the facets dominating the growth morphology have the max growth rate, for the inward growing (concave) situation.

As shown in Figs. 3(b) and 3(e), the sidewall of the holes became vertical and the outer contour of the holes evolved to trapezium or triangle after totally 60 min growth. It illustrates that the six inclined facets are unstable. In addition, some misoriented AlN grew in the holes of sapphire substrate, as marked in the red dotted line circle in Figs. 3(a) and 3(d). Nevertheless, the misoriented AlN appearing in Fig. 3(a) is invisible in Fig. 3(b), deducing that continued growth of the misoriented AlN had been hindered when the inclined facets turned into vertical. As shown in Figs. 3(c) and 3(f), invert V-shaped air gap had been formed when the entire AlN film was nearly coalescent. The reason for the formation of the invert V-shaped air gap might be that the reactant which flowed into the holes was not sufficient for the growth of the lower part of the holes when the opening was small.

This process is quite different from GaN growth on the PSS. As for GaN[28], the entire process of coalescence keeps the symmetrical hexagonal morphology which consisted of the six {11$\bar{2}$2} facets. On the contrary, hexagonal symmetry only existed in the first stage of ELOG-AlN, as mentioned above. One of the possible reasons might be low surface migration of the Al atoms, which means the morphology was influenced mainly by reactant flow rather than surface energy. Also, we believe that the {11$\bar{2}$2} facet was crucial for the symmetrical growth, and it will be discussed later.

Fig. 4 shows the evolution of facets for sample II. The typical morphology with six hexagonal inclined facets after HT-AlN growth for 40 min can be seen in Fig. 4(a). Continuing to react at the condition as HT-AlN will obtain the flat film, thus it can be called the 2D growth mode of the AlN. Conversely, the MT-AlN grown based on HT-AlN reveals no tendency of coalescence, as shown in Fig. 4(b). Growth front of the MT-AlN film is dominated by inclined facets, as the (0001) facet

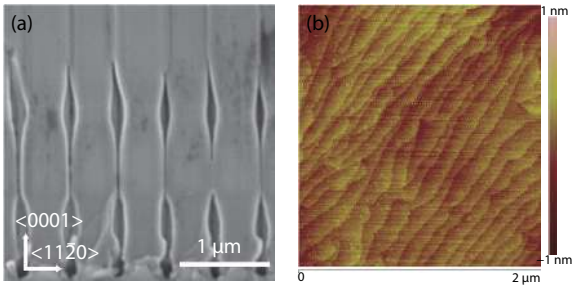

Fig. 6. (Color online) (a) Cross-sectional SEM image and (b) AFM image (2×2 μm^2) of the Sample II after 2D growth.

shrinks and even disappears. Thus the MT-AlN epilayer has 3D growth mode.

Fig. 5(a) shows the tilted-view SEM image of surface morphology after the growth of the MT-AlN, which has been already exhibited in Fig. 4(b). It reveals that the nanoholes with inverse pyramid morphology are well-arrayed. Each hole has nearly closed bottom and six inclined facets. From the cross-sectional SEM image, as shown in the inset of Fig. 5(a), the inclination angle of the facets was measured to be 58°, implying that the facets are {11$\bar{2}$2} type. As mentioned above, the inclined facets are {11$\bar{2}$1} type for the first stage of the HT-

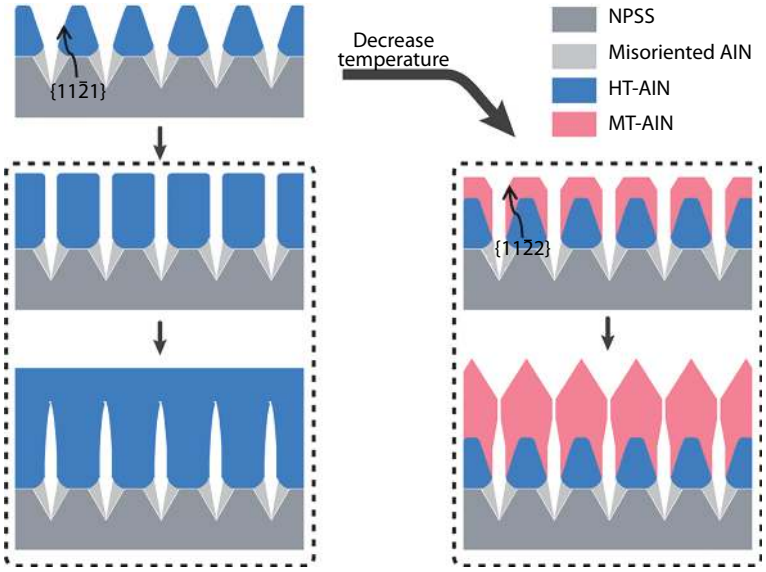

Fig. 7. (Color online) Schematic diagram of the facet evolution of both samples.

AlN. Thus the {11$\bar{2}$2} facets were "induced" by decreasing the growth temperature based on {11$\bar{2}$1} facets. The phenomenon is related to the surface atom of the facets[29]. As shown in Fig. 5(c), the semi-polar {11$\bar{2}$2} facet has the possibilities to be N-terminated or Al-terminated. The N-terminated surface will be passivated with N–H bonds in the growth ambiance of hydrogen[30–32] and hardly accommodate Al adatom, especially for the low growth temperature and N-rich condition (high V/III). Thus the {11$\bar{2}$2} facets with N-polarity which have a low growth rate are stabilized in such growth condition. While for {11$\bar{2}$1} facet, dangling bonds of Al atoms and N atoms both exist in the surface, which is not stabilized, as shown in Fig. 5(d). Stably and slowly growth of the semi-polar {11$\bar{2}$2} facets leads to the inverse pyramid morphology, which can be illustrated in a plain geometrical relationship. Fig. 5(b) is a schematic diagram of the cross section of the hole. v_h represents the vertical growth rate of *c*-plane, and v_s represents the growth rate of the sloped facet. If the point A arrives at the position A′ after a period of growth, the contour lines of the hole evolve from the solid lines to the broken lines. In this case, the relationship of growth rates v_h and v_s needs to satisfy

$$v_s = v_h \cos\theta.$$

Thus if the growth rate of the sloped gets smaller, point A will move left and top facet will shrink. So, the growth velocity of the {11$\bar{2}$2} facets should be below 0.63 μm/h at the growth condition as MT-AlN. Such inverse pyramid structure also can be used for three-dimensional semi-polar LED[33, 34], which is beneficial to reduce the quantum confined stark effect (QCSE) and the efficiency droop, and enhance the LED performance.

In addition, we also tried to realize 2D growth based on MT-AlN. The growth temperature was 1270 °C and the V/III ratio was 578. Flat surface had been obtained after the growth for 2 hours. As shown in Fig. 6(a), the total coalescence thickness was around 2.5 μm. Fig. 6(b) presents a 2×2 μm^2 atomic force microscopy (AFM) image of the surface morphology of the sample II after 2D growth. AlN had a flat surface with a step-flow growth mode and a root-mean-square (RMS) roughness of 0.17 nm.

Another characteristic of the 2D growth based on MT-AlN is that two rows of air gaps in the coalescence region, as shown in Fig. 6(a). The phenomenon is different with typical ELOG of AlN as sample I, which was caused by the behavior of the {11$\bar{2}$1} facets and the {11$\bar{2}$2} facets when grew the MT-AlN. Fig. 7 displays the morphology evolution of the two samples and illustrates the process of forming the air gaps in sample II. As mentioned above, the HT-AlN at the first stage has the inclined facets in {11$\bar{2}$1} type, whereas the as-grown MT-AlN which based on HT-AlN consists of {11$\bar{2}$2} facets. It's necessary to figure out the process how the {11$\bar{2}$1} facets "transform" to {11$\bar{2}$2} facets. As shown in Fig. 7, the {11$\bar{2}$2} facets induced by low temperature in sample II derived from the upper part of {11$\bar{2}$1} facets. The {11$\bar{2}$2} facets become larger after subsequent growth due to the slow growth rate of them-

selves. In the meantime the other part of the $\{11\bar{2}1\}$ facets had the same behavior as the sample I, hence a row of air gaps was formed closed to the substrate. After HT-AlN growth, the 3D structure transformed to 2D smooth surface, another row of air gaps would be formed above the first.

4. Conclusion

We analyzed the morphology evolution of AlN grown on NPSS. We found the process that the $\{11\bar{2}1\}$ type facets emerge and vanish at the relatively high temperature, which illustrates instability of such type facets. And we decreased the growth temperature, inducing the growth of $\{11\bar{2}2\}$ facets and making the growth mode transforms from the initial 2D growth mode to 3D growth mode. In this growth mode, the growth front would get rid of the {0001} type facet. Purely inverse pyramid structure was formed. Also, we implemented the high-temperature growth to transform such inverse pyramid structure to the flat surface, demonstrating temperature plays an important role in the coalescence of AlN. However, the morphology evolution related to the misfit dislocation needs to be further explored.

Acknowledgments

This work was supported by the National Key R&D Program of China (No. 2016YFB0400800), the National Natural Sciences Foundation of China (Grant Nos. 61875187, 61527814, 61674147, U1505253), Beijing Nova Program Z181100006218007 and Youth Innovation Promotion Association CAS 2017157.

References

[1] Ding K, Avrutin V, Özgür Ü, et al. Status of growth of group III-nitride heterostructures for deep ultraviolet light-emitting diodes. Crystals, 2017, 7, 300
[2] Romanov A E, Fini P, Speck J S. Modeling the extended defect evolution in lateral epitaxial overgrowth of GaN: Subgrain stability. J Appl Phys, 2003, 93, 106
[3] Imura M, Nakano K, Kitano T, et al. Microstructure of epitaxial lateral overgrown AlN on trench-patterned AlN template by high-temperature metal-organic vapor phase epitaxy. Appl Phys Lett, 2006, 89, 221901
[4] Kim M, Fujita T, Fukahori S, et al. AlGaN-based deep ultraviolet light-emitting diodes fabricated on patterned sapphire substrates. Appl Phys Express, 2011, 4, 092102
[5] Dong P, Yan J, Wang J, et al. 282-nm AlGaN-based deep ultraviolet light-emitting diodes with improved performance on nano-patterned sapphire substrates. Appl Phys Lett, 2013, 102
[6] Lee D, Lee J W, Jang J, et al. Improved performance of AlGaN-based deep ultraviolet light-emitting diodes with nano-patterned AlN/sapphire substrates. Appl Phys Lett, 2017, 110, 191103
[7] Chen Z, Qhalid Fareed R S, Gaevski M, et al. Pulsed lateral epitaxial overgrowth of aluminum nitride on sapphire substrates. Appl Phys Lett, 2006, 89, 081905
[8] Nakano K, Imura M, Narita G, et al. Epitaxial lateral overgrowth of AlN layers on patterned sapphire substrates. Phys Status Solidi A, 2006, 203, 1632
[9] Imura M, Nakano K, Narita G, et al. Epitaxial lateral overgrowth of AlN on trench-patterned AlN layers. J Cryst Growth, 2007, 298, 257
[10] Mei J, Ponce F A, Fareed R S Q, et al. Dislocation generation at the coalescence of aluminum nitride lateral epitaxy on shallow-grooved sapphire substrates. Appl Phys Lett, 2007, 90, 221909
[11] Jain R, Sun W, Yang J, et al. Migration enhanced lateral epitaxial overgrowth of AlN and AlGaN for high reliability deep ultraviolet light emitting diodes. Appl Phys Lett, 2008, 93, 051113
[12] Hirayama H, Fujikawa S, Norimatsu J, et al. Norimatsu J, et al. Fabrication of a low threading dislocation density ELO-AlN template for application to deep-UV LEDs. Phys Status Solidi C, 2009, 6(Suppl 2), S356
[13] Kueller V, Knauer A, Brunner F, et al. Growth of AlGaN and AlN on patterned AlN/sapphire templates. J Cryst Growth, 2011, 315, 200
[14] Kueller V, Knauer A, Reich C, et al. Modulated epitaxial lateral overgrowth of AlN for efficient UV LEDs. IEEE Photonics Technol Lett, 2012, 24, 1603
[15] Knauer A, Kueller V, Zeimer U, et al. AlGaN layer structures for deep UV emitters on laterally overgrown AlN/sapphire templates. Phys Status Solidi A, 2013, 210, 451
[16] Kueller V, Knauer A, Zeimer U, et al. Controlled coalescence of MOVPE grown AlN during lateral overgrowth. J Cryst Growth, 2013, 368, 83
[17] Zeimer U, Kueller V, Knauer A, et al. High quality AlGaN grown on ELO AlN/sapphire templates. J Cryst Growth, 2013, 377, 32
[18] Dong P, Yan J C, Zhang Y, et al. AlGaN-based deep ultraviolet light-emitting diodes grown on nano-patterned sapphire substrates with significant improvement in internal quantum efficiency. J Cryst Growth, 2014, 395, 9
[19] Zhang L, Xu F, Wang J, et al. High-quality AlN epitaxy on nano-patterned sapphire substrates prepared by nano-imprint lithography. Sci Rep, 2016, 6, 35934
[20] Wang T Y, Tasi C T, Lin K Y, et al. Surface evolution and effect of V/III ratio modulation on etch-pit-density improvement of thin AlN templates on nano-patterned sapphire substrates by metal-organic chemical vapor deposition. Appl Surf Sci, 2018, 455, 1123
[21] Hagedorn S, Knauer A, Mogilatenko A, et al. AlN growth on nano-patterned sapphire: A route for cost efficient pseudo substrates for deep UV LEDs. Phys Status Solidi A, 2016, 213, 3178
[22] Conroy M, Zubialevich V Z, Li H, et al. Epitaxial lateral overgrowth of AlN on self-assembled patterned nanorods. J Mater Chem C, 2015, 3, 431
[23] Beaumont B, Bousquet V, Vennegues P, et al. A two-step method for epitaxial lateral overgrowth of GaN. Phys Status Solidi A, 1999, 176, 567
[24] Hiramatsu K, Nishiyama K, Onishi M, et al. Fabrication and characterization of low defect density GaN using facet-controlled epitaxial lateral overgrowth (FACELO). J Cryst Growth, 2000, 221, 316
[25] Horibuchi K, Kuwano N, Miyake H, et al. Microstructures of two-step facet-controlled ELO-GaN grown by MOVPE method — effect of mask geometry. J Cryst Growth, 2002, 237, 1070
[26] Vennegues P, Beaumont B, Bousquet V, et al. Reduction mechanisms for defect densities in GaN using one- or two-step epitaxial lateral overgrowth methods. J Appl Phys, 2000, 87, 4175
[27] Du D, Srolovitz D J, Coltrin M E, et al. Systematic prediction of kinetically limited crystal growth morphologies. Phys Rev Lett, 2005, 95, 155503
[28] He C, Zhao W, Zhang K, et al. High-quality GaN epilayers achieved by facet-controlled epitaxial lateral overgrowth on sputtered AlN/PSS templates. ACS Appl Mater Interfaces, 2017, 9, 43386
[29] Hiramatsu K, Nishiyama K, Motogaito A, et al. Recent progress in selective area growth and epitaxial lateral overgrowth of III-nitrides: Effects of reactor pressure in MOVPE growth. Phys Status Solidi A, 1999, 176, 535
[30] Li S, Wang A. GaN based nanorods for solid state lighting. J Appl Phys, 2012, 111, 071101
[31] Zhao L X, Yu Z G, Sun B, et al. Progress and prospects of GaN-based LEDs using nanostructures. Chin Phys B, 2015, 24, 068506
[32] Tian Y, Yan J, Zhang Y, et al. Formation and characteristics of AlGaN-based three-dimensional hexagonal nanopyramid semi-polar multiple quantum wells. Nanoscale, 2016, 8, 11012
[33] Wunderer T, Feneberg M, Lipski F, et al. Three-dimensional GaN for semipolar light emitters. Phys Status Solidi B, 2011, 248, 549
[34] Wunderer T, Wang J, Lipski F, et al. Semipolar GaInN/GaN light-emitting diodes grown on honeycomb patterned substrates. Phys Status Solidi C, 2010, 7, 2140